LASer **C**avity
Analysis & **D**esign

Computational Physics Approaches
to Model Solid-State Laser Resonators

Konrad Altmann

LAS-CAD GmbH, Germany

www.las-cad.com

I will talk about four Approaches:

- **Gaussian Mode ABCD Matrix Approach**

- **Dynamic Multimode Approach**

- **Physical Optics Beam Propagation Method based on the Principle of Fox and Li**

The Gaussian Mode ABCD Matrix Approach

Computation of the transverse modes by the use of the Gaussian Mode ABCD Matrix Approach is **very fast and powerful**. It delivers in many cases results which are in good agreement with measurements. This has been proved by many users of the program LASCAD.

As known textbooks of lasers, beam propagation through a series of parabolic optical elements can be described by the use of ABCD matrices. In many cases the optical elements in a resonator, such as spherical mirrors and dielectric interfaces, can be approximated parabolically.

The ABCD Matrices for mirrors, lenses, and dielectric interfaces are well known. I am showing some examples

Mirror

$$M_{Mirror} = \begin{bmatrix} 1 & 0 \\ -2/R & 1 \end{bmatrix}$$

Thin Lens

$$M_{Lens} = \begin{bmatrix} 1 & 0 \\ -1/f & 1 \end{bmatrix}$$

Dielectric Interface

$$M_{Curved\ dielectric\ inderface} = \begin{bmatrix} 1 & 0 \\ (n_2 - n_1)/R & 1 \end{bmatrix}$$

Free Space

$$M_{Free\ Space} = \begin{bmatrix} 1 & L/n_0 \\ 0 & 1 \end{bmatrix}$$

The ABCD matrix algorithm can be applied to compute the **propagation of rays**, but also to **transform the so called q Parameter of a Gaussian beam**

$$u(x, y, z) = \frac{1}{n_0 \, q(z)} \exp\left[- jk \frac{x^2 + y^2}{2R(z)} - \frac{x^2 + y^2}{w^2(z)} \right]$$
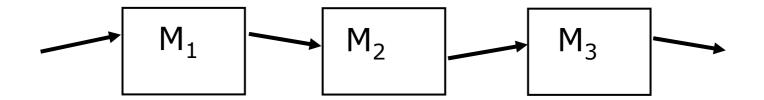
R   radius of the phase front curvature

w   spot size defined as 1/e^2 radius of intensity distribution

The q parameter is a complex quantity and is given by

$$\frac{1}{q} = \frac{n_0}{R} - j\frac{\lambda_0}{\pi\,w^2}$$

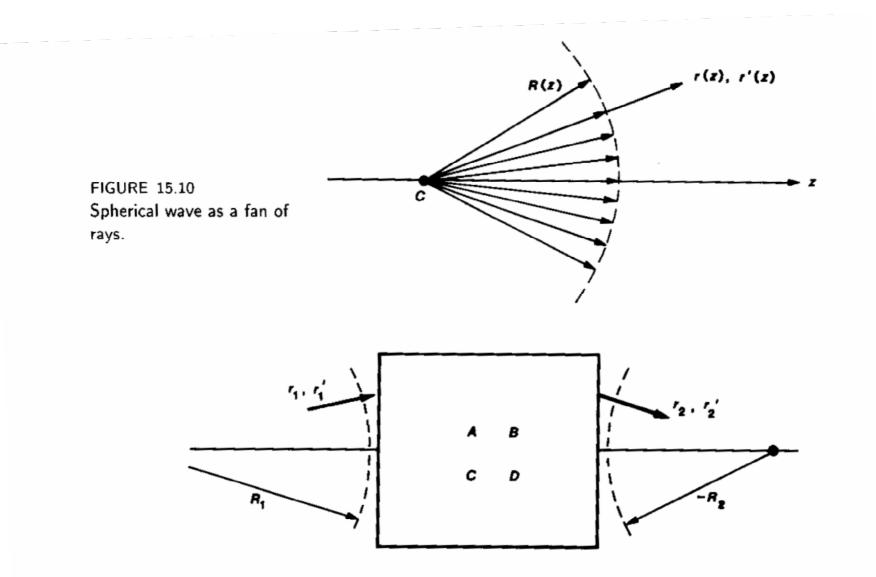The transformation of the q parameter by an ABCD matrix is given by
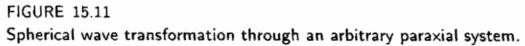
$$q_2 = \frac{A\,q_1 + B}{C\,q_1 + D}$$

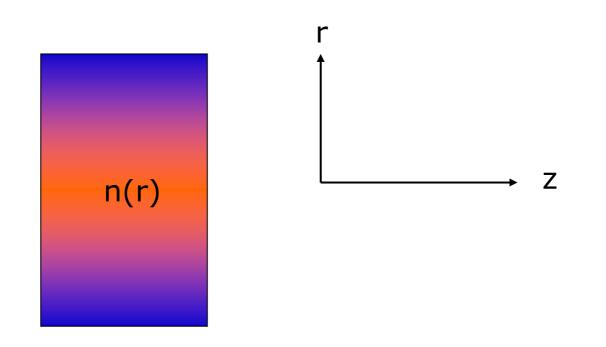ABCD Matrices can be cascaded

The total matrix is given by

$$M_{tot} = M_n \, M_{n-1} \, ... \, M_2 \, M_1$$

FIGURE 15.10
Spherical wave as a fan of rays.

FIGURE 15.11
Spherical wave transformation through an arbitrary paraxial system.

To model thermal lensing the ABCD Matrix of a **Gaussian Duct** is important

A gaussian duct is a transversely inhomogeneous medium whose **refractive index** and **gain coefficient** are defined by parabolic expressions

The **parabolic parameters n$_2$ and α$_2$** of a gaussian duct are defined by

$$n(x) = n_0 - \frac{1}{2} n_2\, x^2$$

and

$$\alpha(x) = \alpha_0 - \frac{1}{2} \alpha_2\, x^2$$

n$_2$ parabolic refractive index parameter

α$_2$ parabolic gain parameter
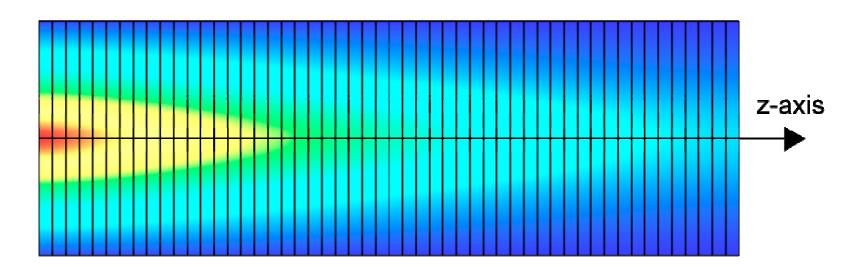
ABCD Matrix of a Gaussian Duct

With the definition

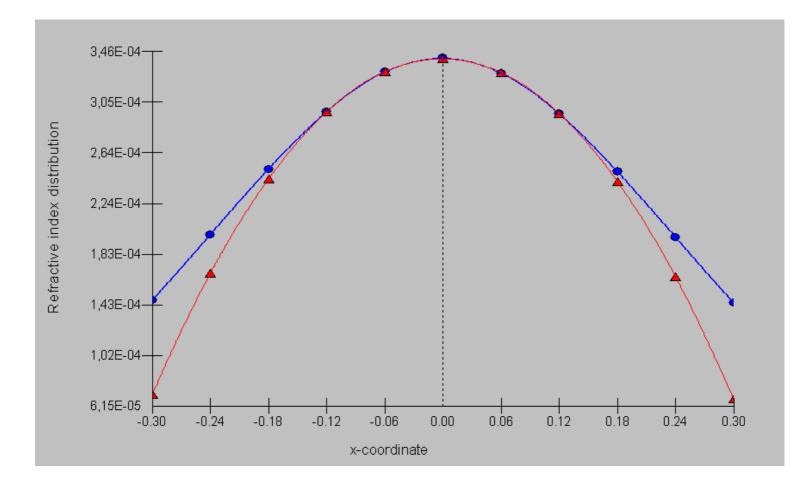$$\gamma^2 = \frac{n_2}{n_0} - j \frac{\lambda_0 \, \alpha_2}{2 \, \pi \, n_0}$$

the ABCD matrix of a gaussian duct can be written in the form

$$\begin{bmatrix} A(z) & B(z) \\ C(z) & D(z) \end{bmatrix} = \begin{bmatrix} \cos\gamma(z - z_0) & \sin(\gamma(z - z_0))/(n_0\gamma) \\ -n_0 \, \gamma \sin\gamma(z - z_0) & \cos\gamma(z - z_0) \end{bmatrix}$$

In LASCAD the concept of the Gaussian duct is used to compute the thermal lensing effect of laser crystals. For this purpose the crystal is subdivided into short sections along the axis. **Every section is considered to be a Gaussian duct**.

z-axis

A parabolic fit is used to compute the parabolic parameters for every section.
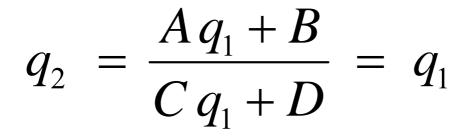

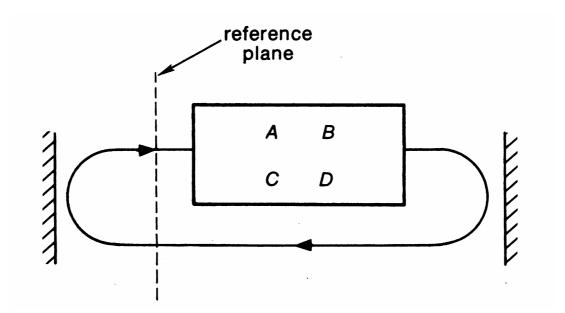Example: Parabolic fit of the distribution of the refractive index

For every section of the crystal an ABCD matrix is computed

With the ABCD matrices of mirrors, lenses, dielectric interfaces, and Gaussian ducts many of the real cavities can be modeled.

To compute the eigenmodes of a cavity the q parameter must be self-consistent, that means it must **meet the round-trip condition**.

Round-Trip Condition

$$q_2 = \frac{A\,q_1 + B}{C\,q_1 + D} = q_1$$

reference plane

A   B

C   D

The **round-trip condition** delivers a simple quadratic equation for the q parameter.
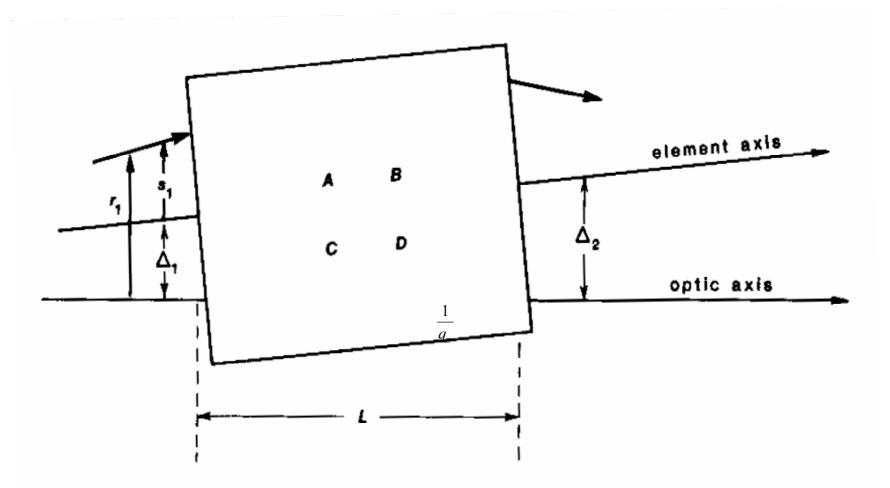
$$\frac{1}{q_a}, \frac{1}{q_b} = \frac{D-A}{2B} \mp \frac{1}{B}\sqrt{\left(\frac{A+D}{2}\right)^2 - 1}$$

All these computations are **simple algebraic operations** and therefore **very fast**.

Gaussian Optics of Misaligned Systems

With 2 x 2 ABCD Matrices only well aligned optical systems can be analyzed. However, for many purposes the analysis of small misalignment is interesting.

This feature has not been implemented yet in the LASCAD program, but it is under development, and will be available within the next months.

FIGURE 15.19
Notation for analyzing a misaligned paraxial optical element.

As shown in the textbook LASERS of Siegman the effect of misalignments can be described by the use of 3x3 matrices

$$
\begin{bmatrix} r_2 \\ r_2' \\ 1 \end{bmatrix} = \begin{bmatrix} A & B & E \\ C & D & F \\ 0 & 0 & 1 \end{bmatrix} x \begin{bmatrix} r_1 \\ r_1' \\ 1 \end{bmatrix}
$$

Here E and F describe the misalignmet of the element

To provide a time dependent analysis of multimode competition and Q-switched operation of lasers we have developed the code DMA
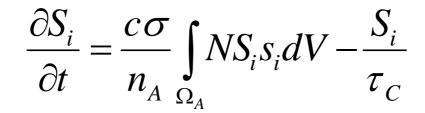
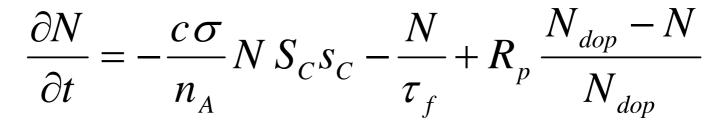## Dynamic Analysis of Multimode and Q-Switched Operation (DMA)

The present DMA code uses the transverse eigenmodes obtained by the gaussian ABCD matrix approach. However, DMA also can use numerically computed eigenmodes.

In the present code the transverse mode structure in the cavity is approximated by a set of M Hermite-Gaussian (HG) or Laguerre-Gaussian (LG) modes.

Since HG and LG modes represent **sets of orthogonal eigenfunctions** with different eigenfrequencies, we assume, that **each transverse mode oscillates independently**, and therefore the influence of short-time locking and interference effects between the modes is neglected on the average. This delivers the following

Multimode Rate Equations

$$S_C = \sum_{i=1}^{M} S_i \qquad i=1,\dots,M$$

$$\frac{\partial S_i}{\partial t} = \frac{c\sigma}{n_A} \int_{\Omega_A} N S_i s_i \, dV - \frac{S_i}{\tau_C}$$

$$\frac{\partial N}{\partial t} = -\frac{c\sigma}{n_A} N \, S_C s_C - \frac{N}{\tau_f} + R_p \frac{N_{dop} - N}{N_{dop}}$$

$S_i(t)$ number of photons in transverse mode i
$S_C(t)$ total number of photons in the cavity
$s_{i,C}(x,y,z)$ normalized density distribution of photons

n_A refractive index of the active medium

c vacuum speed of light

$N(x,y,z,t) = N2 - N1$ population inversion density ($N1 \sim 0$)

$R_P = \eta_P P_a / h\nu_P$ pump rate

η_P pump efficiency

$P_a(x,y,z)$ absorbed pump power density

σ effective cross section of stimulated emission

τ_C mean life time of laser photons in the cavity,

τ_f spontaneous fluorescence life time of upper laser level

N_{dop} doping density.

$\widetilde{L}$

An important quantity is the mean life time τ_C of the laser photons in the cavity. It is given by

$$\tau_c = \frac{t_{rtrip}}{L_{\mathrm{Re}\,s}} = \frac{2\widetilde{L}}{c(L_{roundtrip} - \ln(R_{out}))}$$

where

L_{RES} overall resonator losses

$\widetilde{L}$ optical path length of the cavity

t_{rtrip} period of a full roundtrip of a wavefront

$L_{roundtrip}$ round trip loss

R_{out} reflectivity of output mirror

To obtain the normalized photon densities s_i (i=C; 1,…,M) the complex wave amplitudes $u_i(x,y,z)$ are normalized over the domain $\Omega=\Omega_{2D}\times[0,LR]$ of the resonator with length L_R. Here the u_i (i=1,…,M) denote the amplitudes of the individual modes, whereas u_C denotes the amplitude of the superposition of these modes In our incoherent approximation the absolute square of this superposition is given by

$$\left|u_C(x,y,z)\right|^2 = \sum_{i=1}^{M}\left|u_i(x,y,z)\right|^2$$

The amplitudes u_i and the normalized photon distributions s_i are connected by the following relation

$$s_i = \begin{cases} \dfrac{n_A}{V_i}\left|u_i\right|^2 & \text{inside the crystal} \\[2em] \dfrac{1}{V_i}\left|u_i\right|^2 & \text{outside the crystal} \end{cases}$$
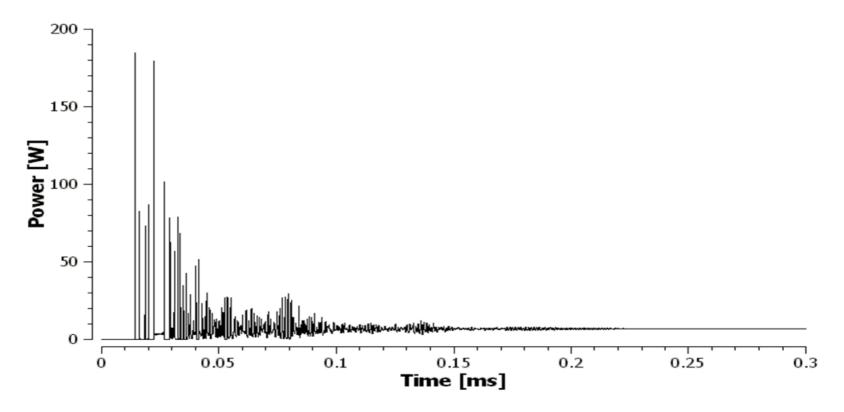
Note that the photon density inside the crystal is by a factor n_A higher than outside due to the reduced speed of light.

Laser Power Output

The laser power output is obtained by computing the number of photons passing the output coupler per time unit. In this way one obtains for the power output delivered by the individual transverse modes
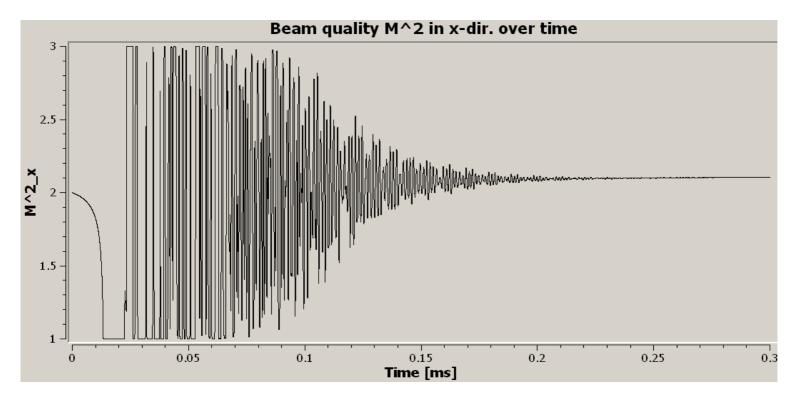
$$P_{i,out}(t) = h\nu_L S_i(t) \frac{-\ln(R_{out})}{t_{rtrip}}\left[1 - 0.5\ln(R_{out})\right]$$

R_{out} reflectivity of output mirror

t_{rtrip} period of a full roundtrip of a wavefront

This plot shows a typical time dependence obtained for the total power output.

Since the computation starts with population inversion density N(x,y,z,t)=0, a spiking behavior can be seen at the beginning, which attenuates with increasing time.

Beam quality M^2 in x-dir. over time

This plot shows a typical time dependence obtained for the beam quality.

Again the spiking at the beginning is caused by the vanishing inversion density N(x,y,z,t) at the start of the computation.

Modeling of Q-Switched Operation

Time dependence of active Q-switching is cha-racterized by three time periods which can be described as follows:

- load period – period I
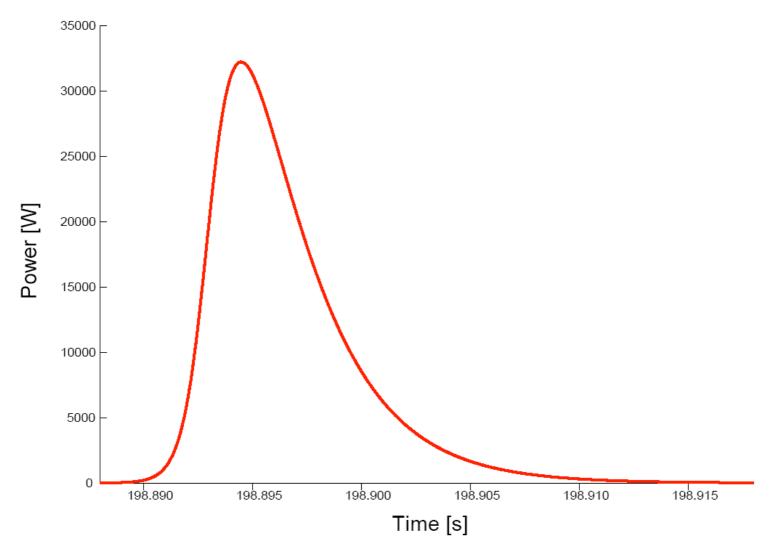- pulse period – period IIa
- relaxation period – period IIb

Development of population inversion and laser power during these periods is shown schematically in this plot

To prevent lasing during the load period a high artificial intra-cavity loss is introduced

After the load period this artificial loss is removed that means the Q-switch is opend and the pulse can develop.

A typical pluse shape obtained with our DMA code is shown on the next slide.

Typical pulse shape computed with the DMA Code

Apertures and Mirrors
with Variable Reflectivity

Apertures and output mirrors with variable reflectivity can be taken into account in the **DMA** by introducing specific losses L_i for the individual modes.
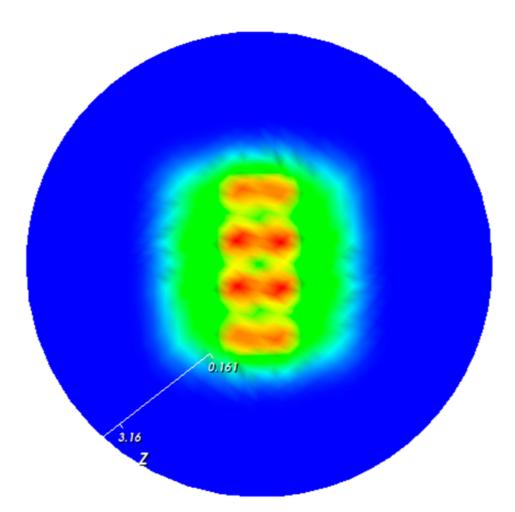
An important realisation of mirrors with variable reflectivity are supergaussian output mirrors. The reflectivity of such mirrors is described by

$$R(x, y) = R_0 \exp\left(-2\left|\frac{x}{w_{trx}}\right|^{SG} -2\left|\frac{y}{w_{try}}\right|^{SG} \right) + R_{min}$$
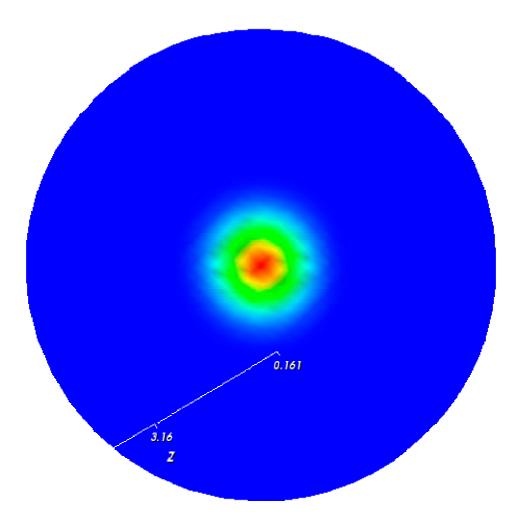
Here R_{min} is a peripheral bottom reflectivity.

With supergaussian mirrors the beam quality can be improved considerably without loosing too much power output.

This shall be demonstrated by the following example.

Beam profile without confining aperture.
Power output 6.87 W

0.161

3.16

Z

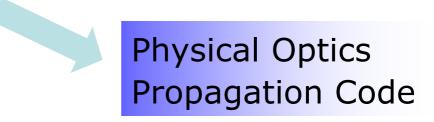Beam profile for the same configuration with supergaussian aperture. Power output 4.22 W

For cases where parabolic approximation and ABCD gaussian propagation code are not sufficient, FEA results alternatively can be used as input for a physical optics code that uses a FFT Split-Step Beam Propagation Method (BPM).

The physical optics code provides full 3-D simulation of the interaction of a propagating wavefront with the hot, thermally deformed crystal, without using parabolic approximation.
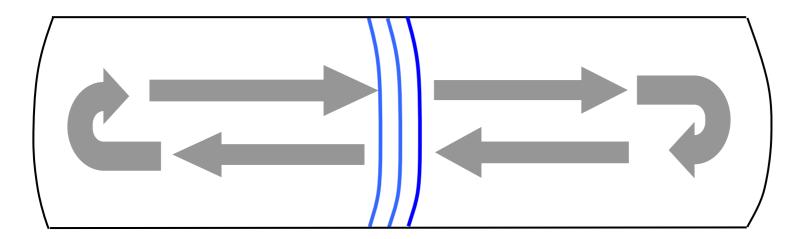
The results of the FEA code of LASCAD can be used with the ABCD gaussian propagation as well as with the BPM physical optics code.

FEA Results:
Temperature distribution
Deformation
Stress

ABCD Gaussian Propagation Code
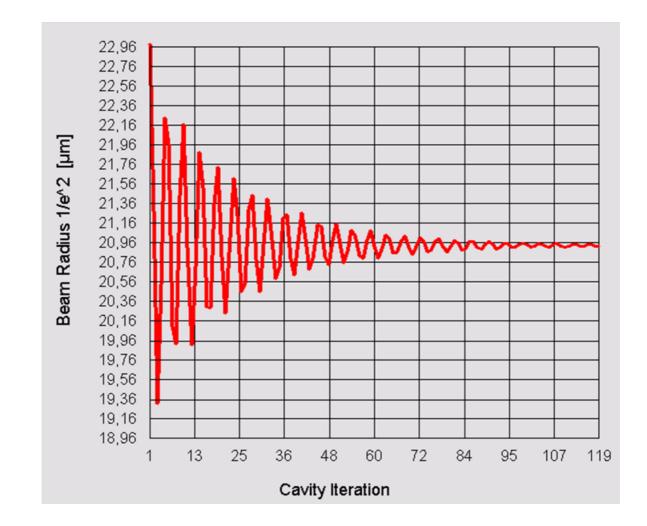
Physical Optics Propagation Code

Based on the principle of Fox and Li, a series of roundtrips through the resonator is computed, which finally converges to the fundamental or to a superposition of higher order transversal modes.

The BPM code propagates the wave front in small steps through crystal and resonator, taking into account the refractive index distribution, as well as the deformed end facets of the crystal, as obtained from FEA.
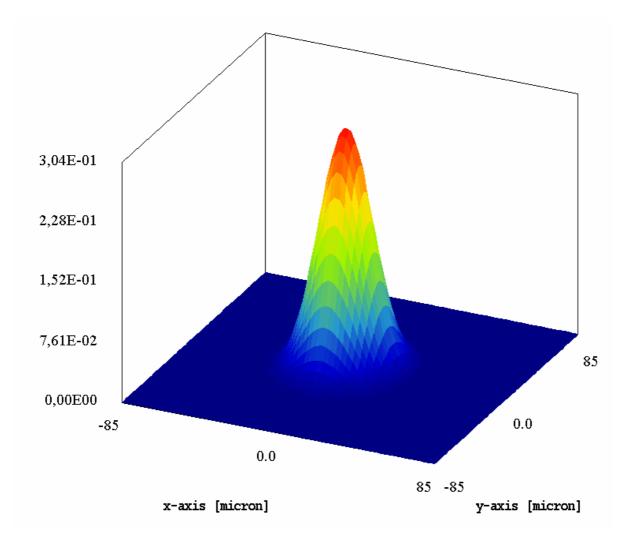
In principle, BPM provides a solution of following integral equation for the electromagnetic field.

$$\gamma \widetilde{E}_{nm}(x, y) = \iint \widetilde{K}(x, y, x_0, y_0) \widetilde{E}_{nm}(x_0, y_0) \, dx_0 dy_0$$
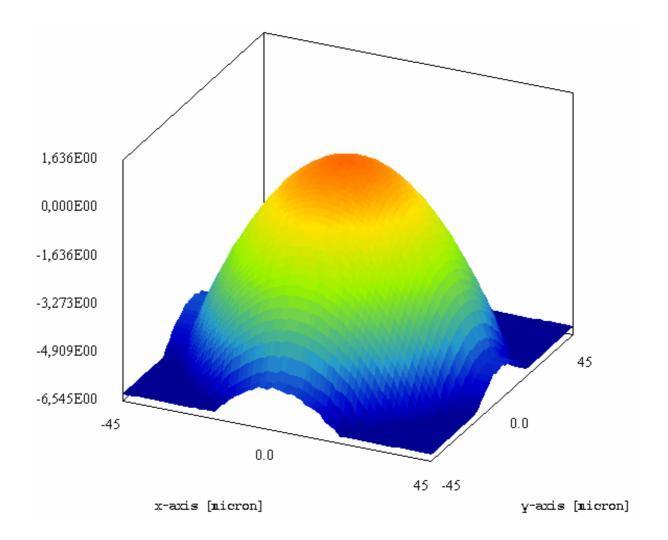
Convergence of spot size with cavity iteration

The wave optics computation delivers realistic results for important features of a laser like intensity and phase profile as shown by the next two slides.
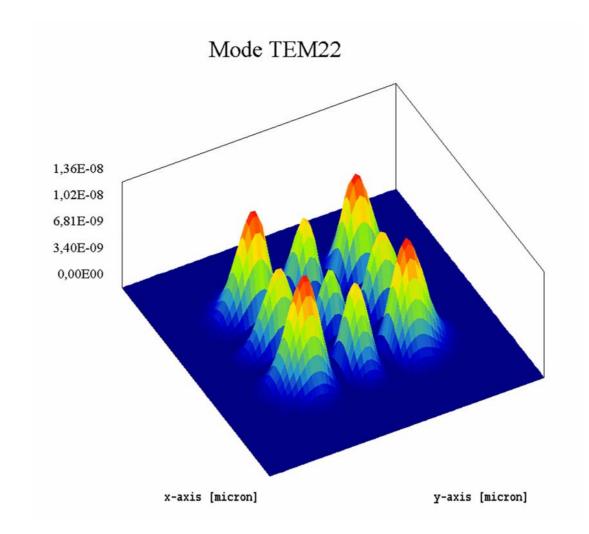
Intensity distribution at output mirror

Phase distribution at output mirror

The BPM code is capable of numerically computing the spectrum of resonator eigenvalues and also the shape of the transverse eigenmodes.

An example for a higher order Hermite-Gaussian mode is shown in the next slide.

Mode TEM$_{22}$ obtained by numerical eigenmode analysis